KAUNAS UNIVERSITY OF TECHNOLOGY
MECHANICAL ENGINEERING AND DESIGN FACULTY

Andrius Kmieliauskas

NUMERICAL ANALYSIS OF SAWDUST TRANSPORTATION

Master's Degree Final Project

Supervisor
Dr. Virginija Gylienė

KAUNAS, 2016

KAUNAS UNIVERSITY OF TECHNOLOGY
MECHANICAL ENGINEERING AND DESIGN FACULTY

NUMERICAL ANALYSIS OF SAWDUST TRANSPORTATION

Master's Degree Final Project
Industrial Engineering and Management (621H77003**)**

Supervisor
(signature) Dr. Virginija Gylienė
(date)

Reviewer
(signature) Dr. Martynas Ubartas
(date)

Project made by
(signature) Andrius Kmieliauskas
(date)

KAUNAS, 2016

KAUNAS UNIVERSITY OF TECHNOLOGY

Mechanical engineering and design faculty
(Faculty)

Andrius Kmieliauskas
(Student's name, surname)

Industrial Engineering and Management 621H77003
(Title of study programme, code)

"Numerical analysis of sawdust transportation"

DECLARATION OF ACADEMIC INTEGRITY

30 May 2016
Kaunas

I confirm that the final project of mine, **Andrius Kmieliauskas**, on the subject "Numerical analysis of sawdust transportation" is written completely by myself; all the provided data and research results are correct and have been obtained honestly. None of the parts of this thesis have been plagiarized from any printed, Internet-based or otherwise recorded sources; all direct and indirect quotations from external resources are indicated in the list of references. No monetary funds (unless required by law) have been paid to anyone for any contribution to this thesis.

I fully and completely understand that any discovery of any facts of dishonesty inevitably results in me incurring a penalty under procedure effective at Kaunas University of Technology.

(name and surname filled in by hand) *(signature)*

Kmieliauskas, Andrius. Pjuvenų transportavimo skaitinis tyrimas. Magistro baigiamasis projektas / vadovas dr. Virginija Gylienė; Kauno technologijos universitetas, Mechanikos inžinerijos ir dizaino fakultetas.

Studijų kryptis ir sritis: Gamybos inžinerija, Technologijos mokslai.

Reikšminiai žodžiai: *buldozeris, skiedros, baigtinių, elementų, metodas.*

Kaunas, 2016. 42 p.

SANTRAUKA

Daugelis pirmaujančių Europos šalių energijos gamyboje vis aktyviau naudoja savus energetinius resursus – biokurą. Lietuvos energetikos ateitis siejama būtent su šia ūkio sritimi.

Įmonė „First Opportunity“ investuoja į biokuro gamybinės bazės ir resursų plėtrą. Ši kompanija nuolat atnaujina ir modernizuoja savo techninę bazę, kuri leidžia surinkti ir paruošti naudojimui daugiau biokuro žaliavos.

Žiemą biomasės transportavimui neigiamos įtakos turi šaltis ir drėgmė. Sudrėkusias ir sušalusias pjuvenas tampa daug sunkiau transportuoti iki konvejerio.

Šiame darbia siekiama optimizuoti buldozerio kaušo geometriją ir nustatyti kaušą veikiančias jėgas. Darbo tikslas – sumoduliuoti buldozerio kaušą, kuris leistų ekonomiškiau transportuoti sušalusią biomasę.

Kmieliauskas, Andrius. Numerical Analysis of Sawdust Transportation: Master‘s thesis / supervisor dr. Virginija Gylienė. The Faculty of Mechanical engineering and design, Kaunas University of Technology.

Study area and field: Production and Manufacturing Engineering, Technological Sciences.

Key words: bulldozer, sawdust, FEM, stress analysis, static analysis.

Kaunas, 2016. 42 p.

SUMMARY

Most of European countries that are leading in energy generation increasingly use their own energy resources – biofuels. Future energetics of Lithuania is precisely linked with this agricultural area.

Company “First Opportunity” invests into production base and resource development of biofuel. The company constantly upgrades and modernizes its technical base, which allows to gather and to prepare greater quantities of raw material.

In winter time transportation of biomass is negatively affected by frost and moisture. Than timber chips moisten and get frosted becomes much more difficult to transport it to conveyor line.

In this work geometry of bulldozer bucket will be optimized. Lighter bucket lets bulldozer move more economic.

Content

Introduction

Environmental and energy-related issues have become fundamental at the global scale and there is a strong need to develop energy-saving and environmentally friendly technologies in all fields of engineering. Most of European countries that are leading in energy generation increasingly use their own energy resources – biofuels. The future energetics of Lithuania is precisely linked with the pursuit to employ the usage of biomass for heating energy more extensively. The management of energy production from biofuels also involves a number of technological issues to be solved so that the process itself is cost and time efficient, environmentally friendly and workflow-smooth in our climate conditions. One of the challenges reported from this industrial field is the transportation of biomass by the bulldozer to the feeding line in cold and humid weather conditions.

In winter time transportation of biomass is negatively affected by frost and moisture. Than timber chips moisten and get frosted becomes much more difficult to transport it to conveyor line. To improve fuel efficiency, it is important to minimize the energy losses due to a resistance during these processes.

The goal of this master paper is to reduce geometry of bulldozer bucket till margin dimensions that could sustain operating biomass pile due to its different mechanical parameters. To achieve the goal a number of objectives have been raised:

1. to analyse machinery that is used for showing biofuel;
2. to analyse factors that influence density;
3. to model dozer and pile of biofuel with SolidWorks software;
4. to optimize geometry of the bucket;

The object of the research is the interaction between wheel loader and pile of biomass.

The paper consists of introduction, two parts and conclusion. First part provides research of mechanical characteristics of dozer and various influencing properties of biomass. Also computational method for solving this problem was overviewed. In second part solvation of the problem and simulation results were showed. The final part provides conclusions and key outcomes of the research.

1 THE ANALYSIS OF THE TECHNICAL FEATURES OF THE EQUIPMENT USED AND BIOMASS

1.1 Boiler house “First opportunity”

The company “First Opportunity” was founded in 2006, combining the different regions of Lithuania working in the production of biofuels and waste processing plants, "Aviridis”, “Medvija” and “Skiedryne”. Currently “First Opportunity” employs about 100 employees. The headquarters of “First Opportunity” office is located in Vilnius. The company has branches in other three cities.

Successful financial results of “First Opportunity” group are a merit of active investment in the development of biofuel resources and production base. Company's success also contributes to the expanding the range of services. “First Opportunity” constantly upgrades and modernizes its technical base, which allows to gather and to prepare greater quantities of raw material. Their aim is to increase level recycling and to improve the quality of secondary products [1].

Most of European countries that are leading in energy generation increasingly use their own energy resources – biofuels. The energetics of Lithuania is precisely linked with this area. In this way, it does both - increases the energy independence of country and supports their businesses and economy. Currently, the production and the use of biofuel in Lithuania deservedly called one of the most rapidly developing branches of the economy, which makes strong tendency of the country's energy future.

Lithuania produces about 18.1% of its heat energy supply from the biofuels at the moment. The future of this quantity is bound to grow. According to the European Union and the recommendations of the National Energy Strategy, in 2020 the application of biofuel in the energy sector of Lithuania will increase more than double. Currently the network of boiler houses which use biofuel is actively expanding. Presently Lithuania has more than 200 such boiler plants, their total capacity is 610 MW [1].

Fig. 1.1 “First Opportunity” boiler house [1]

Lithuania has a great reserve of biofuel which, unfortunately, is not properly utilized. To absorb spare biofuel, active cooperation of land and forest owners, producers and energetics is necessary.

"First Opportunity" is an active member of the Lithuanian Biomass Energy Association. It regularly initiates various types of projects in biofuel cultivation, collection and production that offer long-lasting cooperation agreements not only in the country but also with international partners of neighbouring countries. The company actively contributes to the development of local renewable fuel market [1].

1.2 Machinery used for biomass transportation by the company

1.1.1. Case 621 F

Company "First Opportunity" subdivision that is located in Kazlu Ruda uses the bulldozer called Case 621 F. This machine has a new Tier 4 Final engine that is using Selective Catalytic Reduction technology. Case 621F is the most powerful and efficient Case wheel loaders. In addition to the upgraded solution of emissions, this workhorse takes economy even further with the fuel-saving features such as auto-idle, auto-shutdown and four programmable power modes that match engine output to the task at hand. The worker controls the machine from a roomy cab that provides industry-leading view of all the work [2].

1.1.2. Productivity

Efficiency is optimized by four power modes, that is matched according to provided task. The Ride Control™ option provides excellent material retention and better machine control when moving over rough terrain. This unit is also available with XT (Tool Carrier) or XR (extended reach) linkage and specialty configurations for even greater versatility and productivity [2].

1.1.3. Fuel efficiency

As the mid-sized wheel loader uses Selective Catalytic Reduction Tier 4 Final technology idle-heavy applications and variable power demands fits the need. After-treatment system allows the machine engine to run at the highest performance, which provides faster throttle response while also maintaining lower temperatures and delivering up to 20% better fuel efficiency over other solutions. No Diesel Particulate Filter regeneration or replacement necessary. Case 621F does not need additional downtime. The engine is secured from

overheating. Fuel savings can be furthered with the standard engine shutdown feature — allowing the owner to limit the idle time of the engine [2].

1.1.4. Comfort

The 621F is one of the quietest and commodious cabs in the industry. The machine has class-leading visibility floor-to-ceiling windows and a low rear hood. Also this model has rear-view camera which improves visibility for an operator even more. And an iso-mount design, dual air filtration system and optional heated, air-ride seat designed to provide operators daylong comfort. Award-winning steering joystick helps to reduce operator fatigue [2].

1.1.5. Serviceability

The tire wear on hard surfaces, along with applications using solid foam-filled tires can be reduced with the optional heavy duty axles with hydraulically locking front differentials. Routine cleaning is a breeze due to the cooling module position that limits debris build-up. Every day check-ups become more easy because of ground-level service checks, eye-level fluid gauges and an electronically lifted rear hood that provides complete engine access [2].

Fig. 1.2 Bulldozer from “First Opportunity” boiler house

1.3 High tipping bucket “IMPLEMEX”

Hydraulic tipping is equipped with the fallowing elements:

- 5 mm steel construction
- Reinforcement under the bucket - 10 mm plates
- Extra reinforcements on the sides
- Replaceable cutting blade with Brinell Hardness of 500, double-sided (bolt mounted)

- Twin tipping cylinders
- Hydraulic hoses only
- Attaching brackets included

Table 1.1 Margin dimensions

Model	*Volume, cm^3*	*Weigh, kg*	*Width, mm*	*Depth, mm*	*Height, mm*
UBH-500	*5500*	*1550*	*2800*	*1600*	*1550*

The technical features of the processing equipment are important for further simulation. Bulldozer bucket will be modelled in this research according to margin dimensions and photos that was taken at companies' warehouse. From the driver of wheel loader, it is known that bulldozer operates in 10 km per hour speed. The bucket is made from 5 mm thick steal.

1.4 Main properties of pile of wood chips

Small trees, branches and the tops of trees are chipped by the shredding machines to produce the biomass. Apart of this biomass is shipped from energy plantations to the boiler houses. Untreated raw material is crushed into the chips of a few centimetres long and wide. Usually it dries out naturally by free storage method in the open air or under some shelter. Such biomass usually has 30-50% humidity. Residual moisture is removed from the fuel when it is burned. Wood chips can be dry and wet. The bulk volume of wood chips is quite big, so that it is most suitable for high-power boiler with the ample storage space.

Most commonly measured biomass is counted and sold in the markets by measurement unit called loose cubic meters because material stacked into shipping containers is supposed to have air gaps. During the storage processes another biomass measurement unit should be taken into account the is bulk density. Bulk density is a property of powders, granules or any other masses of corpuscular or particulate matter. It is defined as the mass of many particles of the material divided by the total volume they occupy. The total volume includes particle volume, inter-particle void volume, and internal pore volume. Bulk density is not an intrinsic property of material. It can vary depending on how the material is handled. For example, wood chips poured into some container will have a particular bulk density. When the container is shook, wood chips will move and usually settle closer together, resulting in a higher bulk density. For this reason, the bulk density of powders is usually reported as freely settled.

For experimentation processes normal density is used. For the determining the mass of wood fibre, it is necessary to take very thin samples of absolutely dry wood. The set the weight it is not so difficult. It is much more difficult to determine the volume of the sample. For such purposes a

device as volumetre is used, which determines the volume displaced by the sample liquid or gas volume. Accuracy depends on what state of measuring material is used: a liquid or gas. Most accurately volume is determined using the volume toluene with mineral oil or inert gas - Helium whose unique molecules can penetrate well into the smallest pores-capillaries.

Another factor that influences the density of wood chips is moisture. During the experimentation processes it has been found that biomass with moisture from 40% to 50% has the best combustion properties. The surprising fact is that during different seasons of year the biomass with the same moisture gains different density Fig. 1.3. Also the density of wood chips can differ because of many other factors like: a kind of trees, a part of the trees, further or closer to the centre of a bole, the growth and harvesting conditions and impurities. The mixed biomass was used to gain these experimental results.

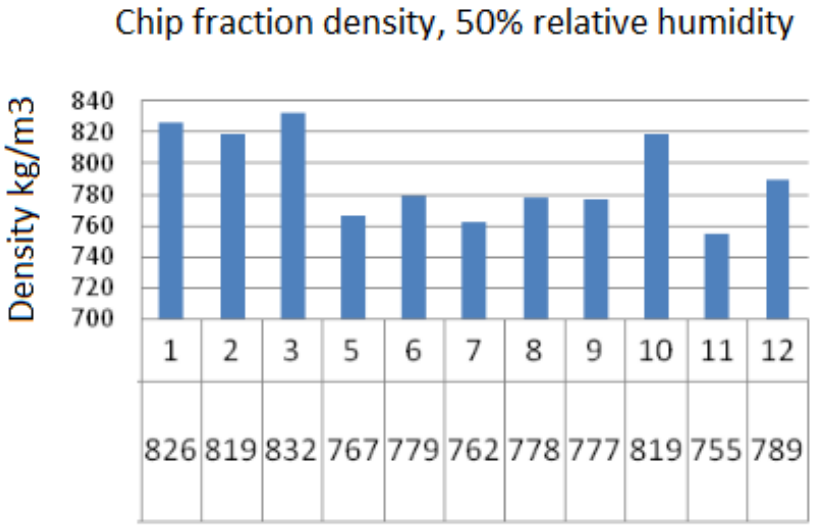

Fig.1.3 Variation of chip fraction density, 50% relative humidity [3]

Another very important property of wood chips for this work is a cohesion rate. It is the property of material sticking together, being mutually attractive. It is an intrinsic property of a substance that is caused by the shape and structure of its molecules that lets orbiting electrons irregularly move when molecules get close to one another. In other words, the cohesion allows for the surface tension of a wood chips pile to create a solid-like state. As we can see in Fig. 1.4, during winter season the cohesion rate is higher, because a pile of wood chips got frozen into a single stack.

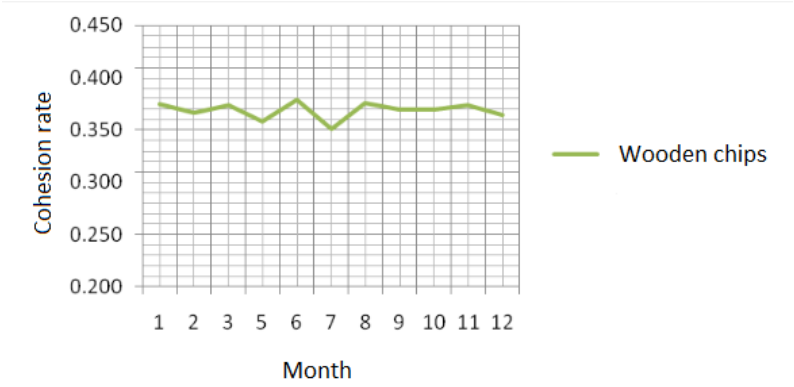

Fig.1.4 Cohesion rate of wooden chips in a relation with the month of the year [3]

1.5 Bulk density

The soil bulk density is the weight of dry soil divided by the volume of the soil. The total soil volume is the combined volume of solids and pores which may contain air or some liquid, or both. The average values of air, water and solid in the soil are easily measured and are a useful indication of the physical condition of the soil. Soil bulk density and the number of pore spaces reflect the size, shape and arrangement of particles and the soil structure [4].

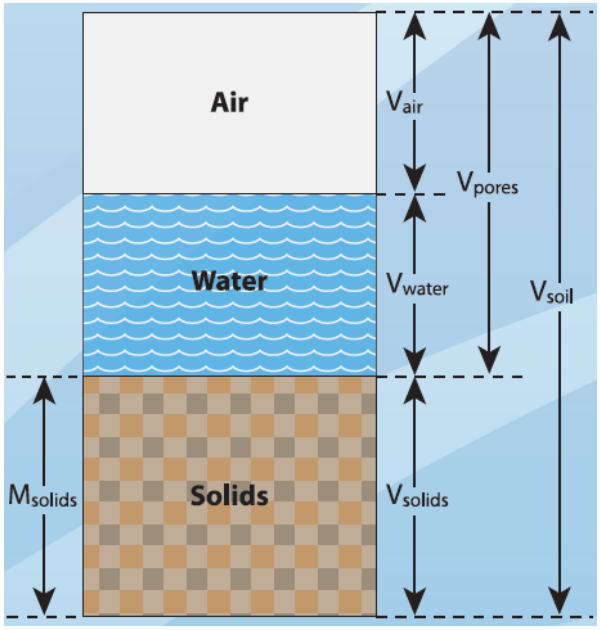

Fig 1.5 Structural composition of soil [4]

2 COMPUTATIONAL METHODOLOGY FOR SIMULATION OF THE PROBLEM

2.1 Finite element method (FEM)

The finite element method (FEM) is a numerical model created to solve problems that are determined with boundary conditions with differential equations. This method is also called finite element analysis. Finite element method split up a large problem into small ones. These subdivided problems that are modelled by finite elements are then joined into a single complicated system of equations that describes all the problem. Various methods from the equations of variations are calculated to minimize error functions.

Advantages of dividing complex problem into smaller division:

- precise model of complex geometry,
- ability to use several different materials in same problem;
- much easier to present general problem;
- more accurate results are gain.

Partial differential equations (PDE) are often used as original equations, that are used to solve complex equations. The equations are usually used to calculate local simple problems. The process from algebraic point of view is to build an inner product integral add the weight functions and set the integral to zero. In short, it is an operation that reduces the errors of the calculation by fitting process functions into the PDE. This procedure excludes all the spatial derivatives from the partial differential equations, thus calculation made locally with the PDE:

- a set of algebraic function that are created for static problems solvation,
- a set of regular differential equations for temporary problems.

Sets of equations consist of element equations. If partial differential equation is linear, then the set of equation are linear also. Algebraic sets of equations for the static problems are solved by numerical linear methods. Regular differential sets of equation used for temporary problems are calculated by the techniques that was presented by Euler.

It is simpler to understand the processes of finite element method from the practical application, that is called finite element analysis (FEA). Finite element analysis is used for mechanical engineering as a computational problem solving tool. This analysis begins with mesh generation techniques used to divide a complex problem into subdivisions.

Finite element analysis is used to analyse complicated problems such as cars strains and oil pipelines, when a solid state is in contact with a changing boundary conditions. For forehead bump simulation analysis lets to increase accuracy of the results in so called important areas. For example,

if car get forward crash it is not necessary to have smooth result of rear part of the car. Also this lets to reduce process cost for the simulation.

2.2 Smoothed-particle hydrodynamics method (SPH)

Smoothed-particle hydrodynamics method would be used to calculate deformation of wood chips pile. In case pile is made of big set of various size and density granules finite element model could not be used. To count accurate mass and the force that would be gain via cutting process between pile and bulldozer bucket knife smoothed-particle hydrodynamics method have to be used.

Smoothed-particle hydrodynamics (SPH) is another computational method used to simulate fluid flows. It was developed by Gingold and Monaghan in 1977. As they started they were developing a method which would help to solve astrophysical problems. Later it was discovered that this approach can be successfully used in many other fields like: astrophysics, ballistics, volcanology, and oceanography. It is a mesh-free method where the coordinates move with the fluid like in Lagrangian formulation. The resolution of the method can easily be adjusted with respect to variables such as the density.

The key principle of the SPH method lies in the introduction of kernel interpolants for flow quantities with the purpose to convey fluid dynamics by a set of particle evolution equations [8]. SPH method differs from other computational methods in the way that seeking to express multiphase flows, there is no requirement to manage the interface shape as it is done in the grid-based methods. As numerous practical simulations have proved that the SPH approach is well suited to problems with large density differences, free-surfaces and complex geometries. Therefore, the SPH method is mostly applied in the fields of hydro-engineering and geophysics. J. J. Monaghan foresees that it might be possible to use SPH as a research tool in surgery in the nearest future.

The SPH demonstrates a great flexibility and new industries gladly introduce it in their technologies. Nowadays it is a major tool in the special effects and graphics industry when it comes to the creation of video games, films, and video advertising. Up to date medias are full of video graphics where a fluid moves and transforms into bizarre shapes and objects thanks to the creativity of the SPH method [8, 10].

J. J. Monaghan explains that “the equations of motion and properties of these particles are determined from the continuum equations of fluid dynamics by interpolation from the particles. The interpolant can be constructed using analytical functions, and spatial derivatives of the interpolated quantities can then be found using ordinary calculus” [10].

2.3 SPH formulation

The SPH method was invented in opposition to the principles of the finite element method because of the extreme deformation problems. Therefore, in the SPH the particles act on the basis of the computational framework where the leading equations are resolved. This model requires a specific method for calculation, which is shown in following part of the paper [9].

2.2.1. Definitions

The particle estimation of a function is:

$$\Pi^h f(x) = \int f(y) W(x-y,h) dy \tag{1.1}$$

Where W is the kernel function.

The Kernel Function W is defined using the function θ by the relation:

$$W(x,h) = \frac{1}{h(x)^d}\theta(x) \tag{1.2}$$

,

where *d* is the number of space dimensions and *h* is the so-called smoothing length which differs in time and in space.

W(x,h) should be a centrally peaked function. The most common smoothing Kernel used the cubic B-spline which is defined by choosing θ as:

$$\theta(u) = c \times \begin{cases} 1 - \frac{3}{2}u^2 + \frac{3}{4}u^3 & for\ /u/ \leq 1 \\ \frac{1}{4}(2-u)^3 & for\ 1 \leq u \leq 2 \\ 0 & for\ 2 < /u/ \end{cases} \tag{1.3}$$

Where *C* is a constant of standardization that relies on the number of space dimensions.

The SPH method is based on a quadrature formula for moving particles ((xi(t)) where x_{it} is the location of particle *I*, which moves along the velocity *v*.

The particle estimation of a function can be defined by:

$$\Pi^h f(x_i) = \sum_{j=1}^{N} w_j f(x_i) W(x_i - x_j, h) \tag{1.4}$$

where $w_j = \frac{m_j}{\rho_j}$ is the weight of particle. The weight of a particle differs proportionally to the digression of the flow.

Formulation of the Smoothed-particle hydrodynamic implies derivative operator. A particle estimation for the derivative operator must be determined. Before giving the description of this estimation, we determine the gradient of a function as:

$$\nabla f(x) = \nabla f(x) - f(x)\nabla 1(x) \tag{1.5}$$

Where 1 is the unit function.

We can observe the linkage that can define the particle estimation to the gradient of a function:

$$\Pi^h \nabla f(x_i) = \sum_{j=1}^{N} \frac{m_j}{\rho_j} [f(x_j) A_{ij} - f(x_i) A_{ij}] \tag{1.6}$$

where: $A_{ij} = \frac{1}{h^{d+1}} \theta'(\frac{//x_i - x_j//}{h}$

We can also determine particle estimation of the partial derivative $\frac{\partial}{\partial x^a}$:

$$\Pi^h(\frac{\partial f}{\partial x^a})(x_i) = \sum_{j=1}^{N} w_j f(x_j A^\alpha(x_i, x_j)) \tag{1.7}$$

Where A is the operator defined by: $A(x_i, x_j) = \frac{1}{h^{d+1}(x_i, x_j)} \frac{(x_i, x_j)}{//x_i, x_j//} \theta' \left(\frac{//x_i, x_j//}{h(x_i, x_j)} \right)$

A^α is the component α of vector A.

2.2.2. Discrete form of conservation equations

The equation has to be solved:

$$L_v(\emptyset) + divF(x, t, \emptyset) = S \tag{1.8}$$

Where $\emptyset \in R^d$ is the unknown, F^β with $\beta \in \{1..d\}$ is the conservation law L_v. The transfer operator is determined by:

$$L_v : \emptyset \to L_v(\emptyset) = \frac{\partial \emptyset}{\partial t} + \sum_{l=1}^{d} \frac{\partial (v^l \emptyset)}{\partial x^l} \tag{1.9}$$

The estimation of the formula:

It is the beginning of the initial formulation of the equation. The discrete form of this problem implies the definition of the operator of derivation D defined by:

$$D: \emptyset \to D\emptyset(x) = \nabla\emptyset(x) - \emptyset(x)\nabla 1(x) \tag{1.10}$$

The estimation of the particle with its operator is:

$$D_h\emptyset(x_i) = \sum_{j=1}^{N} w_j(\emptyset(x_j) - \emptyset(x_i))A_{ij} \tag{1.11}$$

At last, the discrete form of the formula is written down as:

$$\frac{d}{dt}\left(w_i\emptyset(x_i)\right) + w_i D_h F(x_i) = w_i S(x_i) \tag{1.12}$$

This formula is not conventional and this formulation is not numerically acceptable. So for programming purposes it is appropriate to use a weak form of this function.

The weak formulation estimation

In the weak formulation, the adjoint of the L_v, operator is used:

$$L_v^*: \emptyset \to L_v^*(\emptyset) = \frac{\partial\emptyset}{\partial t} + \sum_{l=1}^{d} v^l \frac{\partial\emptyset}{\partial x^l} \tag{1.13}$$

The discrete form of this operator correlates with the discrete formulation of the adjoint of $d_{h,s}$:

$$D_{h,s}^*\emptyset(x_i) = \sum_{j=1}^{N} w_j(\emptyset(x_j)\, A_{ij} - \emptyset(x_j)A_{ij}) \tag{1.14}$$

A discrete adjoint operator is taken to be the α-th component of the operator:

$$D_\alpha^*\emptyset(x_i) = \sum_{j=1}^{N} w_j\emptyset(x_j)\, A^\alpha(x_i, x_j) - w_j\emptyset(x_i)A^\alpha(x_j, x_i) \tag{1.15}$$

This progression leads to the conventional method. Further the conventional equations that meet the SPH method formulation will be solved by the weak formulation.

2.2.3. Application to conservation equations

According to the derivation of the formulation above, it is possible to proceed working out formulas in their discrete form.

The momentum equation is:

$$\frac{dv^\alpha}{dt}\left(x_i(t)\right) = \frac{1}{\rho_i}\frac{\partial\left(\sigma^{\alpha,\beta}\right)}{\partial x_i}(x_i(t)) \tag{1.16}$$

The particle estimation of the weak form of this equation is

$$\frac{dv^{\alpha}}{dt}(x_i) = \sum_{j=1}^{N} m_j \left(\frac{\sigma^{\alpha,\beta}(x_i)}{\rho_i^2} A_{ij} - \frac{\sigma^{\alpha,\beta}(x_j)}{\rho_i^2} A_{ji}\right) \tag{1.17}$$

Energy conservation equation:

$$\frac{dE}{dt} = -\frac{P}{\rho} \nabla v \tag{1.18}$$

The particle estimation of the weak form of this equation:

$$\frac{dE}{dt}(x_i) = \frac{P_i}{\rho_i^2} \sum_{j=1}^{N} m_j (v(x_j - v(x_i)) A_{ji} \tag{1.19}$$

2.2.4. Formulation Available in LS-DYNA

It is easy from the general formulation displayed in equation 1.14 to enlarge the SPH formulation to a set of equations of discretization for the momentum equation.
To introduce the symmetric smoothing function this equation follows:

$$\frac{dv^{\alpha}}{dt}(x_i) = \sum_{j=1}^{N} m_j \left(\frac{\sigma^{\alpha,\beta}(x_i)}{\rho_i^2} + \frac{\sigma^{\alpha,\beta}(x_j)}{\rho_i^2} A_{ji}\right) \tag{1.20}$$

This is the so called symmetric formulation which is chosen in the *CONTROL_SPH card.
Also we can define the momentum equation by the following formula:

$$\frac{dv^{\alpha}}{dt}(x_i) = \sum_{j=1}^{N} m_j \left(\frac{\sigma^{\alpha,\beta}(x_i)}{\rho_i \rho_j} A_{ij} - \frac{\sigma^{\alpha,\beta}(x_j)}{\rho_i \rho_j} A_{ji}\right) \tag{1.21}$$

This is the “fluid formulation” invoked with IFORM=5 which assures better results than other SPH formulations when fluid material is present, or when materials with very different stiffness are used.

2.2.5. Sorting

In the Smooth-particle hydrodynamic method, the location of neighbouring particles is important. It is necessary to find which particle has interaction with others and at what time it happened. A bucket sort is used to portion the domain into accurate boxes and let them easier to be sorted. With this partitioning the closest neighbours will reside in the same box or in the closest boxes. Sorting method allows a number of distance calculations to be reduced, what leads to make simulations on slower computers.

2.2.6. Artificial viscosity

The artificial viscosity is produced when an impact appears. Function discontinuities occur because of the collision. The purpose of the artificial viscosity is to delicately shock over several particles. The artificial viscous pressure term P_{ij} is added so that:

$$p_i \rightarrow p_i + \Pi_{ij} \tag{1.22}$$

where, $\Pi_{ij} = \frac{1}{\bar{\rho}_{ij}}(-\alpha\mu_{ij}\bar{c}_{ij} + \beta\mu_{ij}^2)$

The notation $\bar{X}_{ij} = \frac{1}{2}(X_i + X_j)$ has been used for median between X_i and X_j, c is adiabatic sound speed, and

$$\mu_{ij} = \begin{cases} \bar{h}_{ij}\frac{v_{ij}r_{ij}}{r_{ij}^2+\eta^2} & if\ v_{ij}r_{ij} < 0 \\ 0 & otherwise \end{cases} \tag{1.23}$$

Here $v_{ij} = (v_i - v_j)$ and $\eta^2 = 0.01\bar{h}_{ij}^2$ which prevent the denominator from vanishing.

First-order scheme for time integration is used. For a single time step we use expression:

$$\delta t = C_{CFL} Min\left(\frac{h_i}{c_i + v_i}\right) \tag{1.24}$$

Where C_{CFL} is a numerical constant factor.

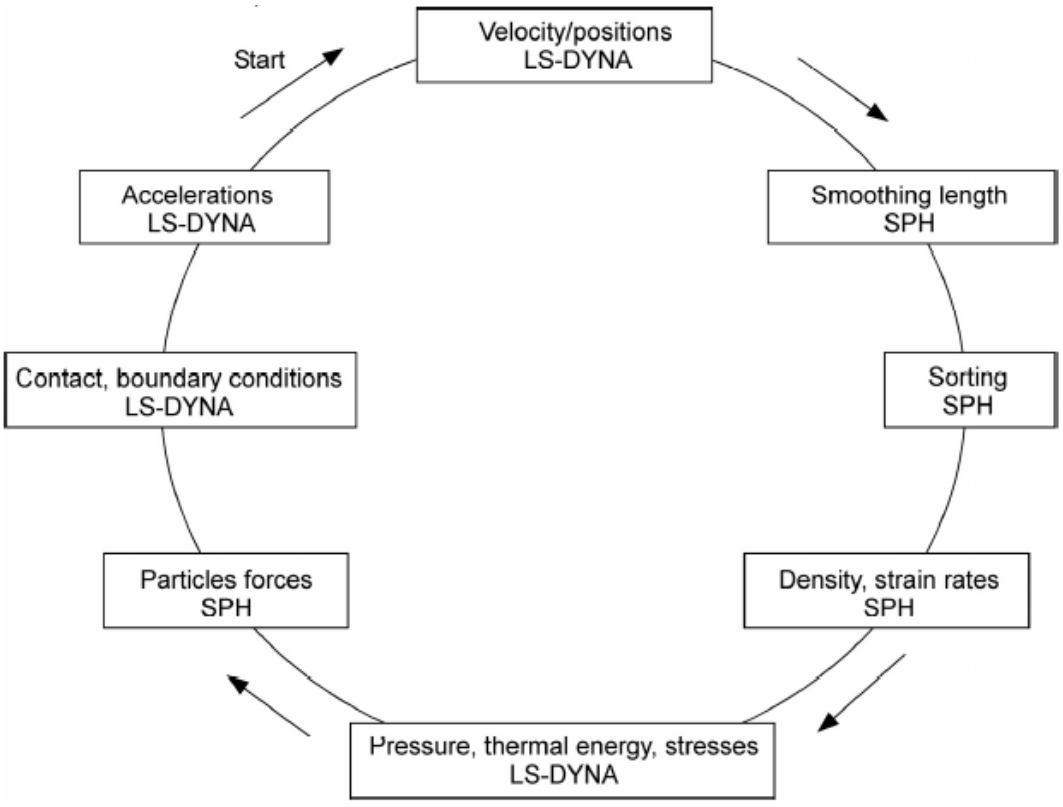

Fig. 1.3 Calculation cycle [9]

2.2.7. Setup of the program

To begin with, physical and geometrical properties of the chosen particle have to be set up into the program. After that, physical properties: mass, density, constitutive laws are defined in the ELEMENT_SPH and the PART cards.

The particles that will be used for the experimentation are placed automatically according to the shape and geometrical properties of the model. Two different parameters: x_i lengths and the C_{SLH} coefficient are defined in the SECTION_SPH card.

The appropriate SPH mesh of the model must meet the following requirements: it must be very simple and must not contain too large variations otherwise it will take a lot of time for the computation.

For a cylinder SPH mesh model, we have at least two variations for particles to be set up:

Fig. 1.4 Cylinder SPH mesh [9]

The Mesh 2 in Fig. 1.4 takes too many different distances between separate particles. Therefore, the Mesh 1is more uniform, more suitable for the computation.

The coupling of finite elements and SPH elements is comprehended by using the contact algorithms. Contact type for particles have to be chosen at „nodes_to_surface“, where the slave part and the master part is defined.

2.4 Granicles in SPH

To make a simulation of a dust storm or a volcanoclastic flow, particulate matter in the SPH code has to be added. The first possibility is to use Harlow & Amsden method [11] and interpret the particular matter as a fluid material that is exposed as air by the means of various forces. Also the same practice was taken by Monaghan & Kocharyan [12], and adapted to simulate dusty rings

around some stars [13]. The main idea is to replace fluid by a set of SPH particles. Every particle represents a large number of dust grains that specify the system, using the SPH particles for the gas or liquid, and SPH boundary particles for the terrain.

Employing smooth particle hydrodynamic method, it is possible to simulate the precipitation of several types of particles with different properties in a stratified fluid. Every set of particles of a fluid with reference parameters like density and friction size can be used for multi-fluid calculations. The different fluids, what is different sets of SPH particles, have their different drag terms as well. Lately soil-water interaction by changing the grain fluid with a very high viscosity was ran. Gained results was quite reasonable [14]. The smoothed particle hydrodynamic method uniquely relates with DEM. The idea is to replace each SPH particle by a set of particles. All group moves like a single particle, also a set of particles translates and rotates like a rigid body. These sets of particles are called "granicles" [15] and are related to the algorithms that use none spherical particles [16]. The shape of the "granicles" can be described as a balloon filled with gas. It can transform its form with a distance that is linked with a set of particles. It may have the corners of a cube or oval shape. If granicles are combined with moderate viscosity it will form piles with a slope that has the shape of the granicles. A mix of fluid (SPH particles) and granicles is called Bingham fluid [15]. Further study of granicles, its behaviour, properties, relations with actual granular material, will be very interesting.

Various problems involving disrupted free surfaces can be easily simulated using the smoothed particle hydrodynamic method and the results are quite satisfactory. The results of the simulation can be more accurate if additional data like surface tension is included.

2.5 Granular material modelling

Ulrich et al. in 2013 proposed visco-plastic rheological model for fluid or granicles flow simulations [17]. This model will be adopted for simulating the movement of the granular materials combined with the SPH method. For computation equations and predicting the shape of the flow, four independent parameters are needed. Most common example is prepared by the Cross with equation [18]:

$$\frac{\mu_0 - \mu}{\mu - \mu_\infty} = (K\gamma)^m \tag{1.25}$$

where K and m are constant values, μ_0 and μ_∞ refer to asymptotic values of viscosity. The shear rate γ, is defined as:

$$\gamma = \sqrt{2\varepsilon^{ij}\varepsilon^{ij}} \tag{1.26}$$

where $\varepsilon^{ij} = \frac{1}{2}\left(\frac{\partial u^i}{\partial x^j} - \frac{\partial u^j}{\partial x^i}\right)$.

In the equation of granular phase, where μ_0 corresponds to the viscosity of solid or elastic limit if γ values are low, while μ_∞ is the viscosity of grains that has high values of γ. We may assume that $\mu \ll \mu_0$, and reduce equation to the Sisko model [19]:

$$\mu = \mu_\infty + \frac{\mu_0}{(K\gamma)^m} = \mu_\infty + K_2\gamma^{n-1} \tag{1.27}$$

Assuming n = 0, we get

$$\mu = \mu_\infty + \frac{K_2}{\gamma} \tag{1.28}$$

which is better known as the Bingham model. By redefining some parameters, we can simplify this model to equation:

$$\tau = \mu_0\gamma + \tau_{yield} \tag{1.29}$$

where τ is the shear stress and τ_{yield} is the yield stress. To describe this model, we can say that some material is assumed as a solid body. Then the shear stress takes higher value than the yields stress, what would result large deformations, material start to be computed as fluid material. One of the commonly used models is the Mohr-Coulomb failure criterion. In this model the shear strength of soil is expressed as a combination of adhesion and friction components [20].

$$\tau_{yield} = c + \sigma^n tan\varphi \tag{1.30}$$

where c is the cohesion, φ is the internal friction angle, while σ^n is the normal stress. However, it is important to note that c and φ are not fundamental properties of material. From previous work of this study, it is sufficiently to assume that *c* and φ are fundamental material constants.

Assuming that σ^n = p, the final form of the granular material model takes the form

$$\mu = \begin{cases} \mu_\infty + \frac{c+\rho tan\varphi}{\gamma}, & \mu < \mu_{solid} \\ \mu_{solid}, & \mu \geq \mu_{solid} \end{cases},$$

where μ_{yield} is added to computational formulation, to avoid extremely high values of viscosity, that lead to extremely small time steps.

2.6 Cohesive bond model

Various simulation for excavation and pushing processes of soil by a bulldozer blade was done by the smoothed particle hydrodynamic method. As we know, usually soil is moistened and the resistance forces acting on the bulldozer blade is largely influenced by the cohesive force. This force appears when soil particles are connected by liquid bridges. One of the cohesive bond force

models was proposed by Utili and Nova [21]. The microscopic behaviour of cohesive force was modelled analogously with macroscopic shear failure characteristics.

In the previous section about SPH granicles, the effect of water content is not included. To get more accurate results of the simulations, a number of models have been developed to determine the cohesive bond force, that occurs due to water content inside. Usually, cohesive bond models are divided into three categories [21]:

I. Models that are very primitive and does not include physical parameters. Despite its importance across the field of study, the modelling of cohesive granular materials is still widely used [21].

II. Models in which liquid-bridge is formed. Cohesive force physical interactions are seen at the microscopic particle-level. In this approach, problems are solved by the Young–Laplace equation for a liquid bridge for paired particles. It is termed as a bottom-up approach. The macroscopic behaviours of cohesive particles are based on the physical interactions at the microscopic particle-level [21].

III. Macroscopic characteristics allow cohesive force to be modelled. Differently from the second category, this approach is termed as a top-down. Mohr–Coulomb failure criterion best describes macroscopic shear characteristics of cohesive materials. Utili and Nova model states that cohesive force at the microscopic particle-level have to be modelled analogously like Mohr–Coulomb failure criterion. We can assume that this approach is good for the solution of problems related with geomechanics sphere, while calibration processes of microscopic model parameters are necessary for the quantitative predictions [21].

3. STATIC SIMULATION

3.1 Modelling of the wood chips pile in SolidWorks

Before modelling pile of wood chips big quantity of information was reviewed. It is necessary to characterise pile of wood chips as much accurate as it is possible to gain results that would be acceptable. Main property of the pile is density. Usually biomass is poured into big piles without vibrating it. To gain more realistic results, bulk density was taken. Volume of the pile is 19 m^3. That volume corresponds the truck which carries biomass from the plant to storage place.

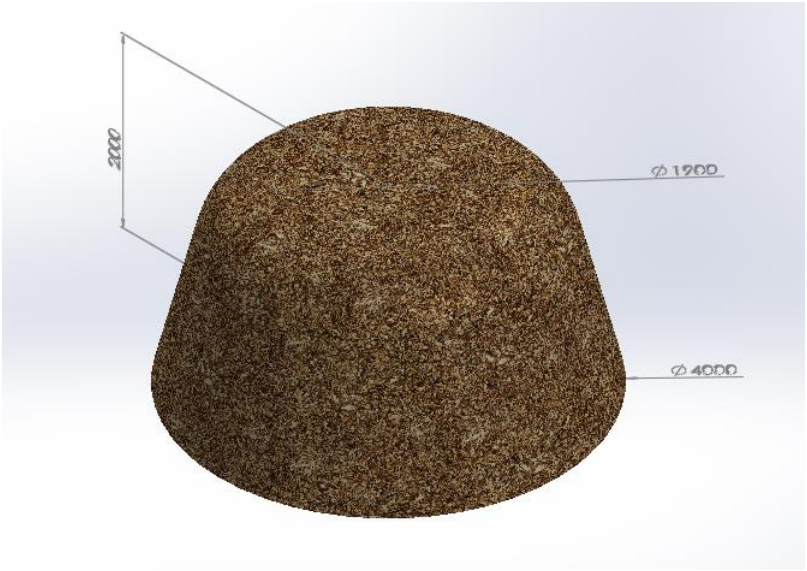

Fig.3.1 Prototype of wood chips pile

By using data from the theoretical analysis forces that are acting on the bulldozer bucket is calculated and presented in Table 3.1.

Table 3.1 Forces interacting bulldozer bucket

Operating volume	4,5 m^3	
Season	Summer	Winter
Humidity	50%	50%
Density	762 kg/m^3	832 kg/m^3
Bulk Density	544 kg/m^3	594 kg/m^3
Mass	2448 kg	2673 kg
Force	24480 N	26730 N

3.2 Modelling of the bucket in SolidWorks

For upcoming simulation models with SolidWorks software was made. The model was done according to the dozer that is used by company “First Opportunity”. According to the photography that was provided by employee of the company and marginal dimensions that are submitted in

“Implemex” distributor page, bulldozer bucket was modelled. As you can see from the Fig. 3.2 several strengthening plates were welded inside the bucket. At the bottom of the dozer knife of mangalloy steel (HB400) was attached. This bucket hinged to bulldozer with fastening connection at the top of the bucket and also hydraulic forks that are used to dispose content of the dozer at bottom of both sides. From the Fig. 3.2 covered bays could be approached.

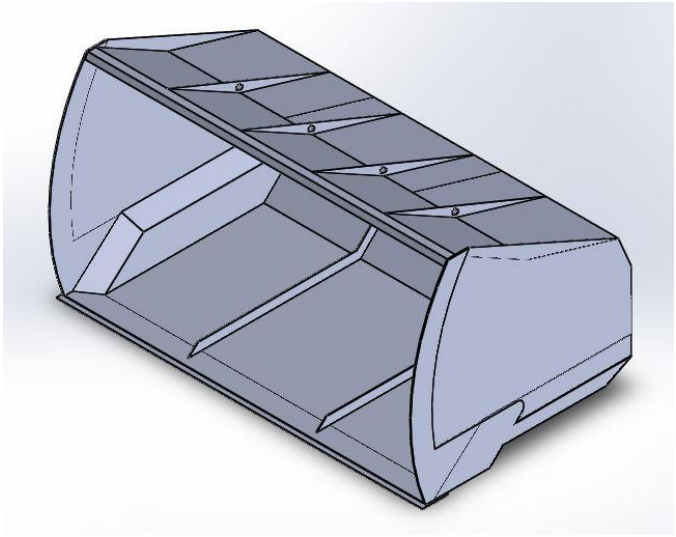

Fig. 3.2 Dozer with strengthening plates

Strengthening constructions are made from 10 mm steel plate. Also sides and top of the bucket are strengthened with additional parts. These fastening elements let bucket to operate greater quantities of materials. For the further simulation these components wont effect the results. To reduce computational time and meshing errors, fastening plates were excluded. Geometry of dozer was simplified, see fig. 3.2.

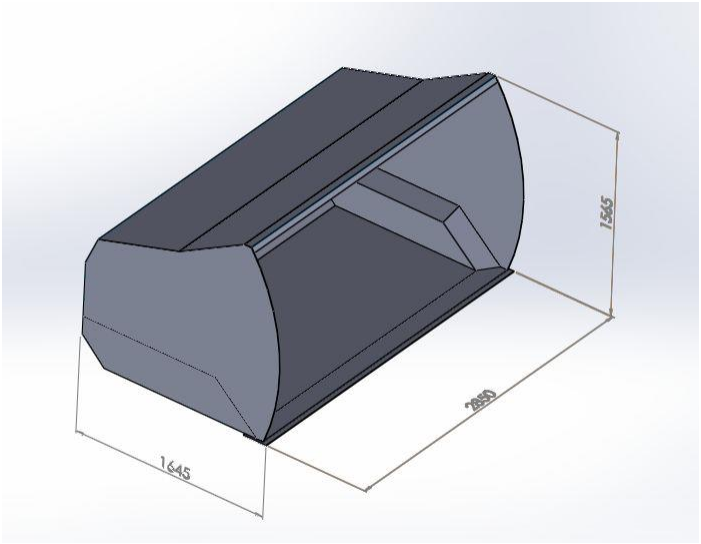

Fig. 3.3 Dozer without fastening

The bucket is 1565 mm high, 2850 mm wide and 1645 mm depth. By using SolidWorks software volume of the bucket was calculated – 5,2 m^3. Because of working behaviour practical capacity of the bucket was reduced 4 m^3.

"Implemex" bucket is made of Steel sheet AISI 316. Mechanical characteristics is shown in Table 3.2. Total mass of the bucket is 795 kg.

Table 3.2 Mechanical properties of Steel sheet AISI 316

Property	Value	Units
Elastic Modulus	1.929999974e+011	N/m^2
Poisson's Ratio	0.27	N/A
Tensile Strength	580000000.8	N/m^2
Yield Strength	172368932.3	N/m^2
Tangent Modulus		N/m^2
Thermal Expansion Coefficient	1.6e-005	/K
Mass Density	8000	kg/m^3
Hardening Factor	0.85	N/A

3.3 Static simulation to determine stiffness of the bucket

To determine stiffness of the bucket multiple static simulations were made. In case biomass has density that varies because of many factors, it is necessary to check the limits that bucket can handle. For static simulations two different densities were used. For pile of wood chips with 50% of moisture in summer – 544 kg/m^3 and for pile with 50% moisture in winter, bulk density of 594 kg/m^3 was taken.

Static simulation was made on bucket with stiffness elements and without it to observe necessity of strengthening constructions of the bucket.

Before running the simulation sequence of operation have to be done. First of all, part should be imported into SolidWorks interface and material of the bucket should be added. Than bucket should be fix by points or in this way by surfaces. Gravity force and force that represents biomass have to be applied. Last step before running the simulation is to mesh the bucket. As thicker mesh is, more accurate results are see Fig. 3.4.

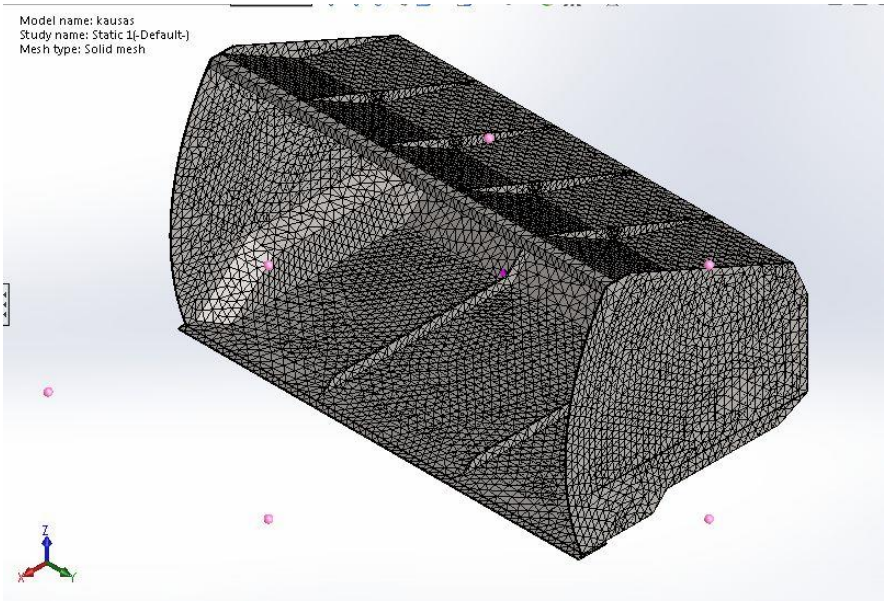

Fig. 3.4 Meshed bulldozer bucket

3.4 Constrains that act on the bucket

Wheel loader connects with the bucket by to hydraulic forks and 4 hinges. Hydraulic forks are located on the sides of the bucket and are covered with steel sheet box. 4 hinges are located on the bottom of the bucket. Green arrows represent the surfaces where the bucket is fixed see Fig. 3.5.

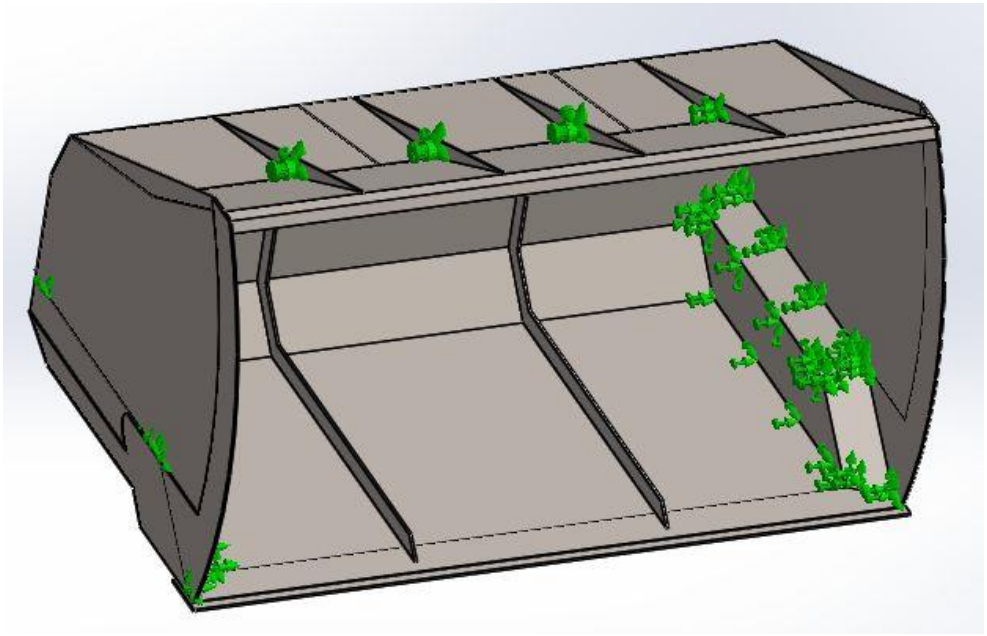

Fig. 3.5 Fixed points of the bucket

In case the highest force acts at the beginning of transportation process, so the load is applied to the bottom surface of the bucket. Only single surface sustains the load force, because

bucket with mass move just in linear motion. Highest deformations will be seen at his surface. Also force of gravity is applied to attach the mass of the bucket into simulation, because it will affect the results of the simulation see Fig. 3.6.

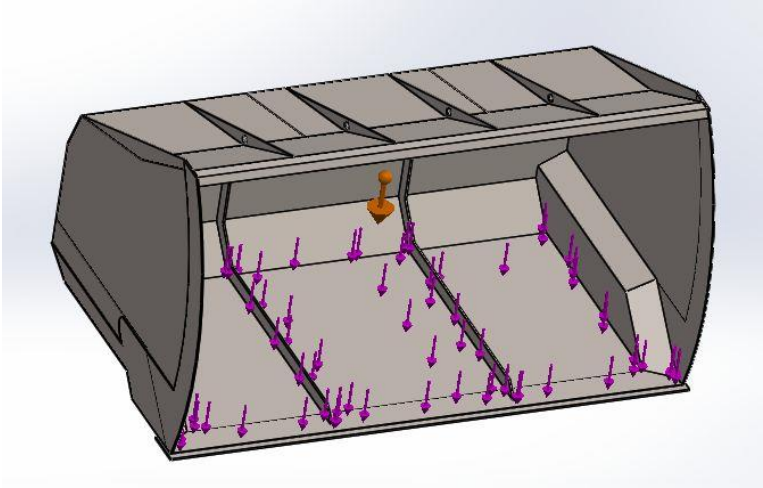

Fig. 3.6 Meshed bulldozer bucket

3.5 Bucket with load of wood chips with 544 kg/m^3 density, influence of strengthening elements

As it was mentioned before, this bucket can operate 4,5 m^3 of material. Force of 24480 N was applied to bottom surface. Middle of surface exposes greatest alteration in displacement. From the simulation results Fig. 3.7 and Fig 3.8 may assume that strengthening elements reduces bucket displacement at peak point more than 4 times. Greatest alteration values of displacement are seen at the middle of the bottom surface.

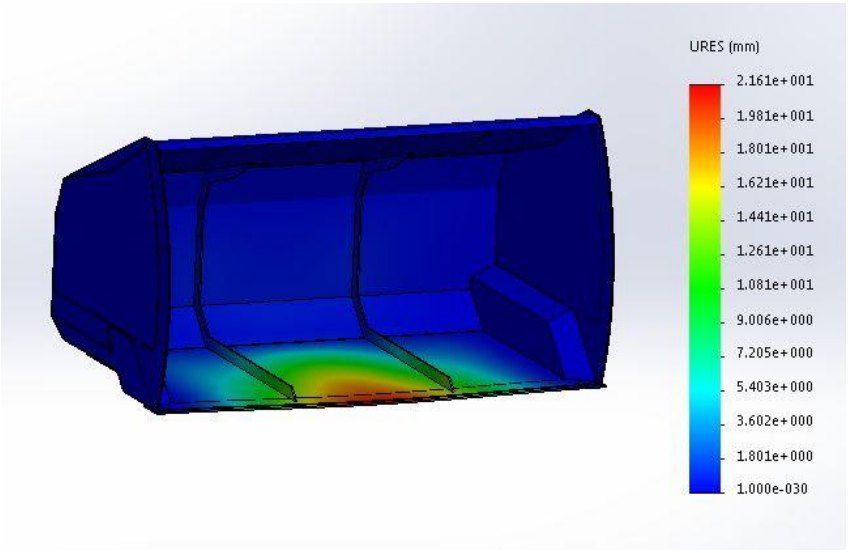

Fig. 3.7 Displacement of bucket with strengthening elements when force of 24480 N is applied

Bucket that does not have strengthening elements reaches 8,6 cm alteration in displacement.

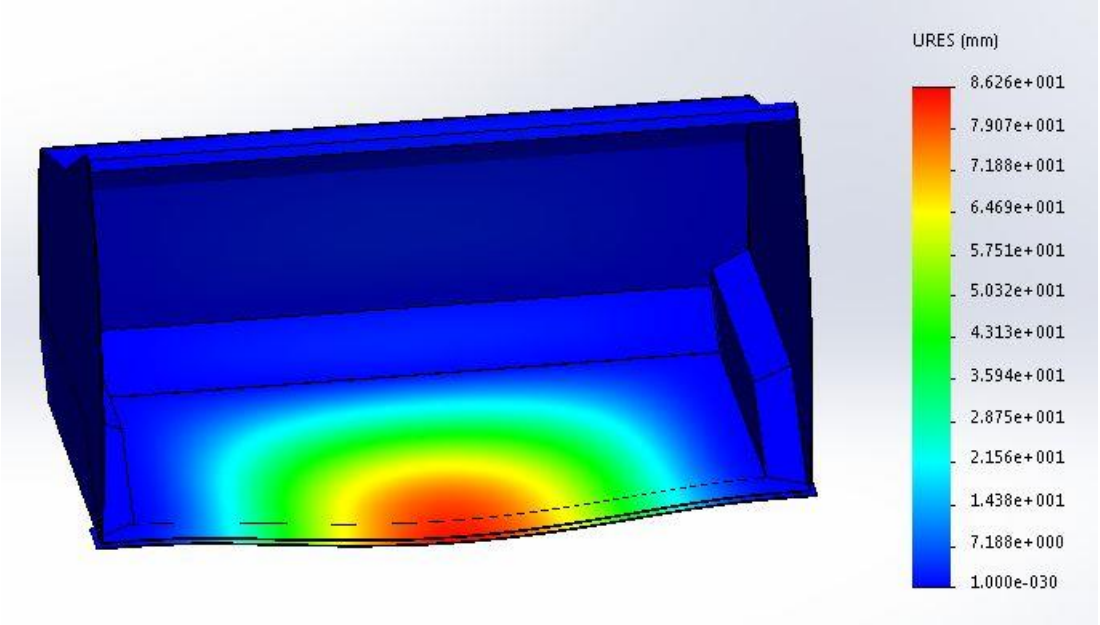

Fig. 3.8 Displacement of bucket without strengthening elements when force of 24480 N is applied

In figures 3.9 and 3.10 we can observe that biggest stresses appear in contact points between strengthening surfaces and bottom surface. Strengthening elements reduces stresses from side walls and reduces peak points almost double. Yield strength limit was not reached fastened case. Bucket is safe from fractures.

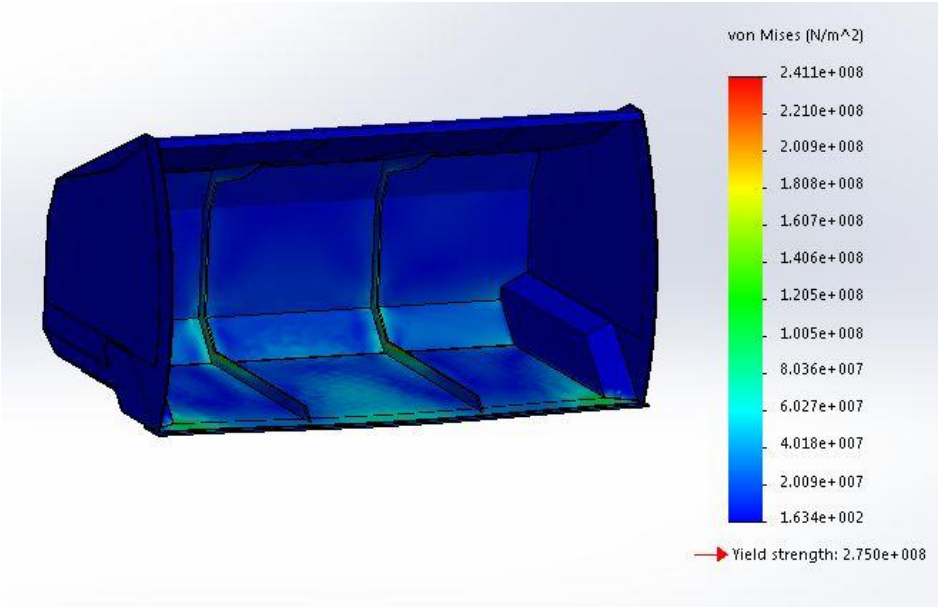

Fig. 3.9 Stress of bucket with strengthening elements when force of 24480 N is applied

Oppositely from Fig. 3.9 bucket that does not have strengthening elements exceeds yield strength limit and bucket sustains irreversible alteration or even fractures. This bucket is not safe to use.

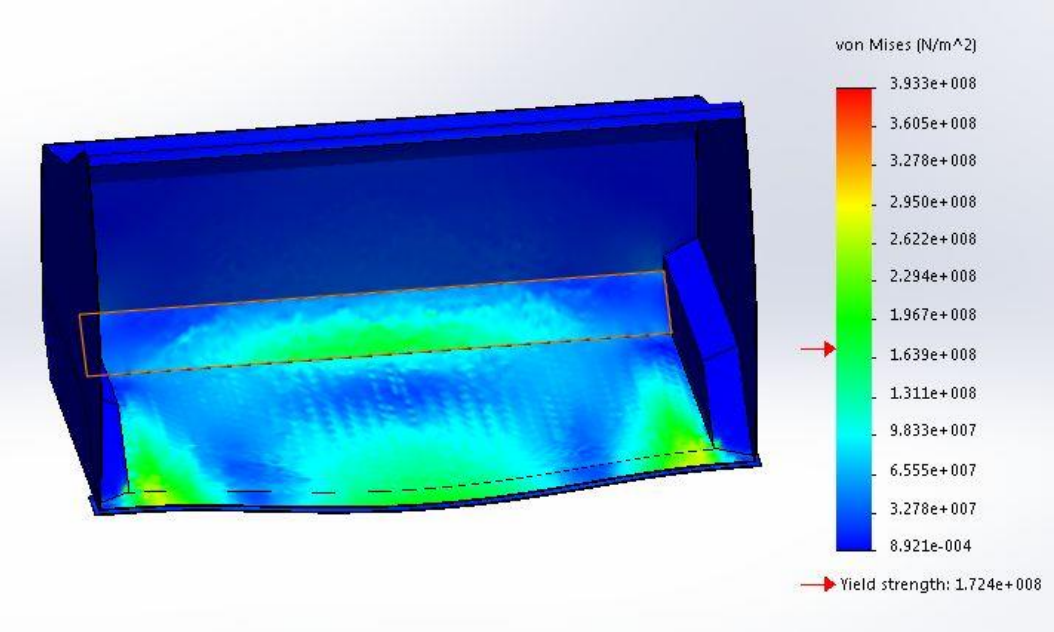

Fig. 3.10 Stress of bucket without strengthening elements when force of 24480 N is applied

Maximum stresses occur at the bottom of the blade in the zone where it connects with hinge box.

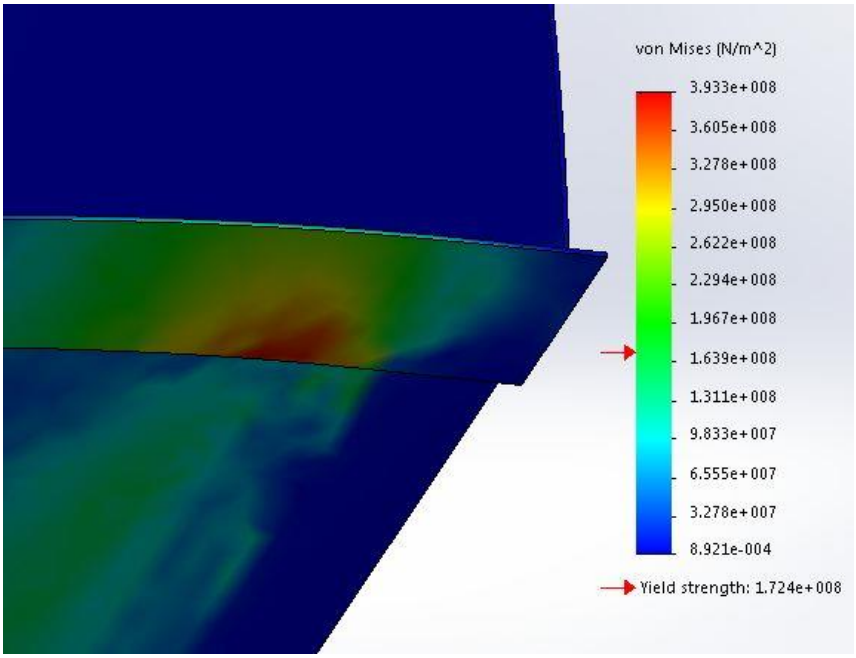

Fig. 3.11 Stress of bucket without strengthening elements when force of 24480 N is applied, maximum stress zone

3.5 Bucket that is used by the company with load of wood chips with 594 kg/m^3 density

Force of 26730 N represents mass of the biomass in winter season. It is applied to bottom surface of the bucket. In fig. 3.12 maximum displacement reached 23 mm. The purpose of this simulation is to find out if universal bucket that is used by the company can sustain load that are operated in winter time without any significant damage of the bucket.

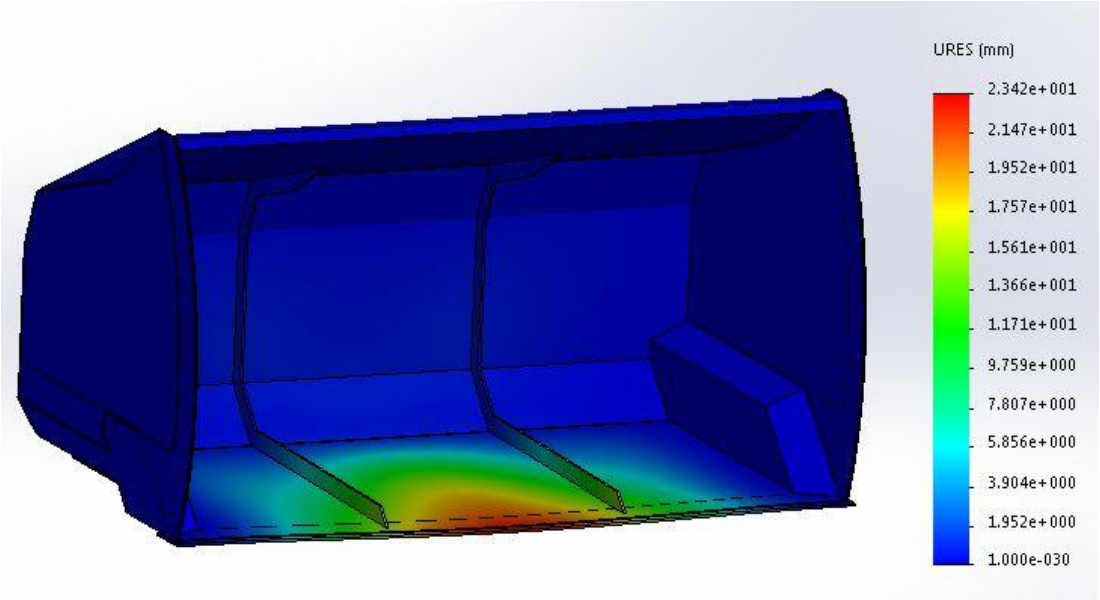

Fig. 3.12 Displacement of bucket with strengthening elements when force of 26730 N is applied

Bucket with stiffness components almost reached yield strength limit, but still it is safe to use, see Fig. 3.13. If wood chip pile with greater density wood be carried with that bucket, it would probably have ended up with a fracture.

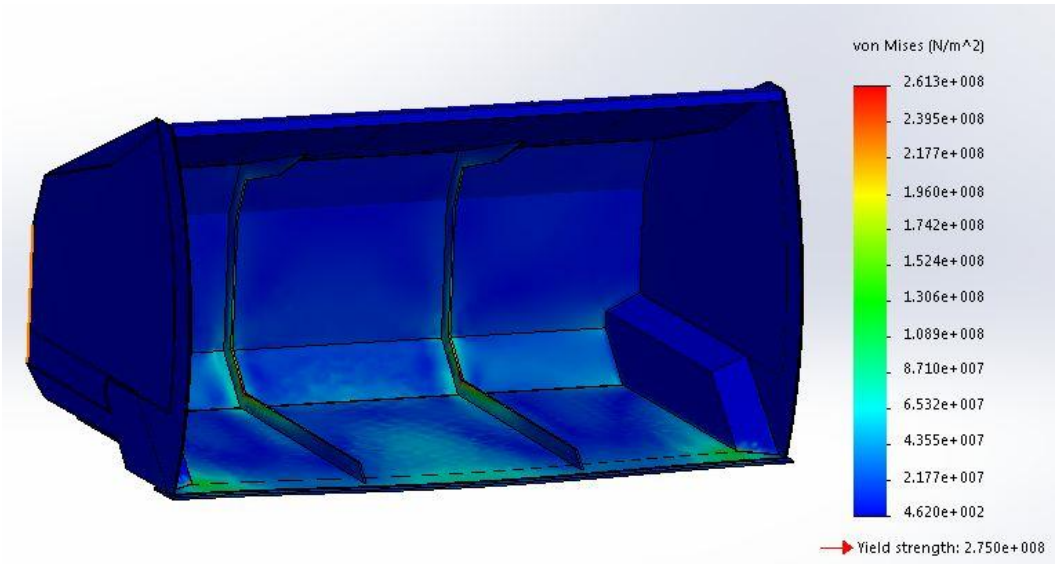

Fig. 3.13 Stress of bucket with strengthening elements when force of 26730 N is applied

In the Fig. 3.14 it is shown that greatest stresses occur at the strengthening elements. That means that fastening elements absorb stresses from the sides of the bucket.

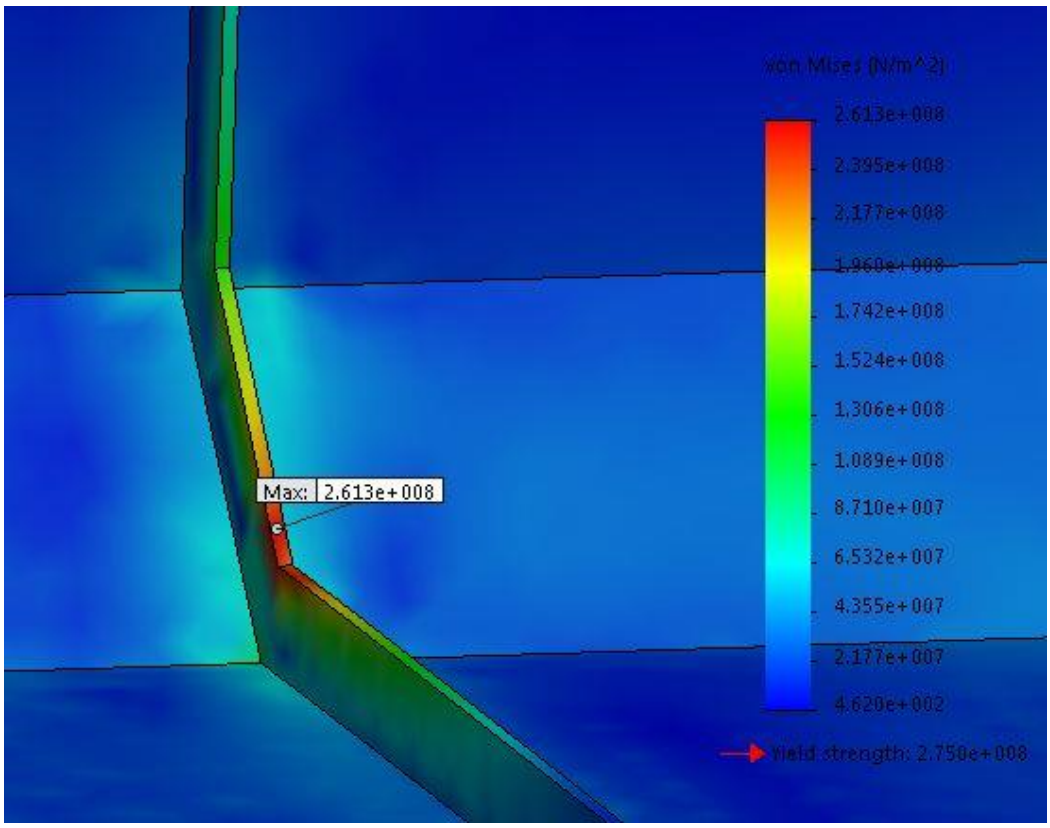

Fig. 3.14 Stress of bucket with strengthening elements when force of 26730 N is applied maximum stress zone

At Fig. 3.15 mass properties of the bucket is presented. Density of the steel is 8000 kg/m^3. The mass of the bucket is almost 800 kg.

Mass properties of kausas
Configuration: Default
Coordinate system: -- default --

Density = 8000.00 kilograms per cubic meter

Mass = 795.29 kilograms

Volume = 0.10 cubic meters

Surface area = 33.94 square meters

Center of mass: (meters)
X = 1.31
Y = 0.77
Z = 0.69

Fig. 3.15 Mass properties of 6 mm thickness bucket

3.6 Bucket of 4 mm thickness steel sheet with load of 24480 N force

To reduce mass of the bucket and to make it operate more efficient thickness of bucket walls was reduced from 6 mm to 4 mm. It is necessary to run the simulation and check if the bucket can sustain operating stresses.

Stresses does not exceed the limit and bucket is safe from fractures Fig. 3.16.

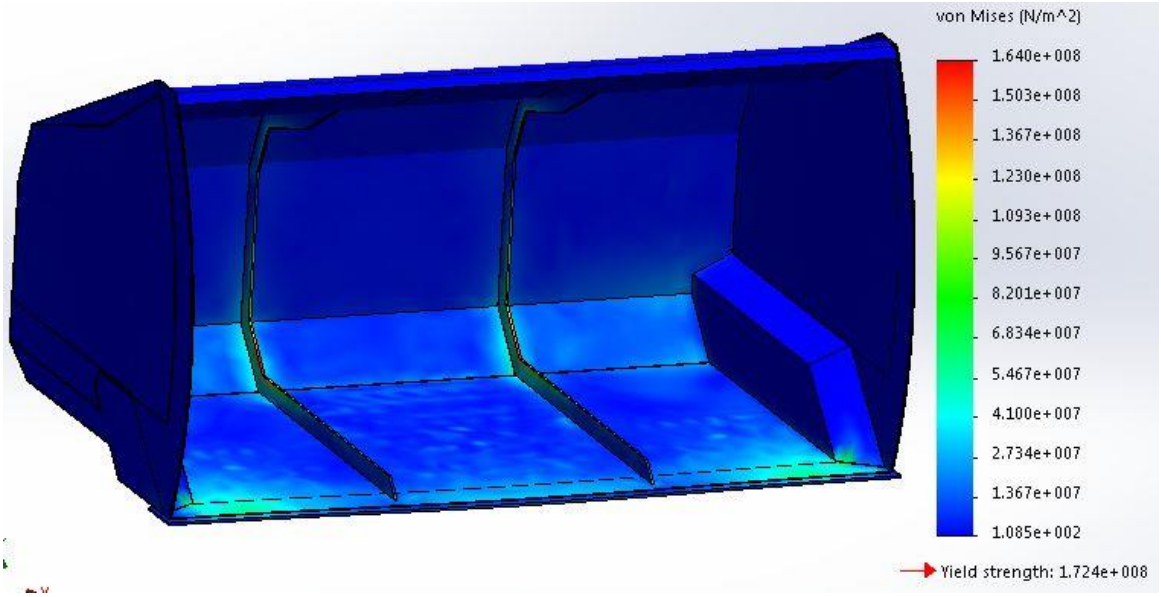

Fig. 3.16 Stress of 4 mm thickness bucket with strengthening elements when force of 24480 N is applied

Displacement of the bucket alters only by 14 mm. Bucket is safe to use with this load.

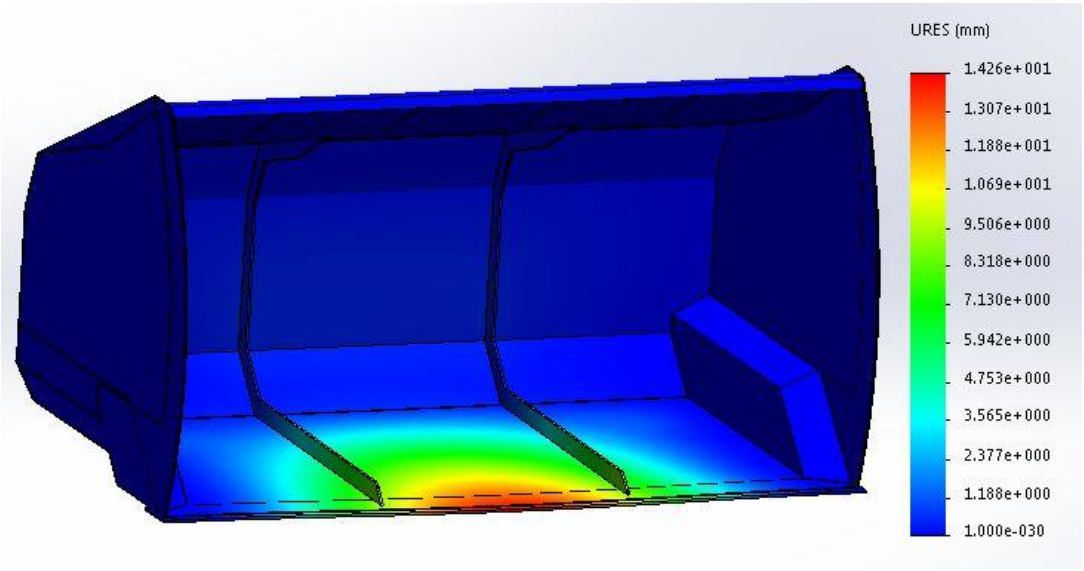

Fig. 3.17 Displacement of 4 mm thickness bucket with strengthening elements when force of 24480 N is applied

3.7 Bucket of 4 mm thickness steel sheet with load of 26730 N force

Load of 26730 N force is applied to bottom surface of the bucket. This force occurs in winter season than density of biomass becomes greater. Thickness of the bucket walls is 4 mm.

In the Fig. 3.18 it is observed that stresses exceed yield strength and bucket is too weak for the operating mass. Operation would end with fracture.

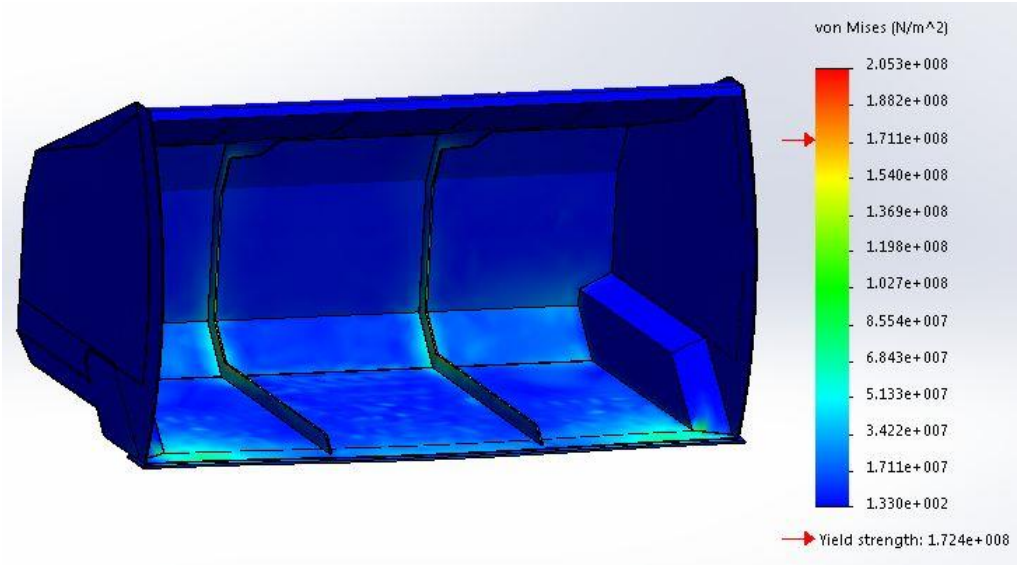

Fig. 3.18 Stress of 4 mm thickness bucket with strengthening elements when force of 26730 N is applied

Maximum stress occurs at the strengthening elements. Yield stress is exceeded by $0{,}333*10^8$ N/m^2.

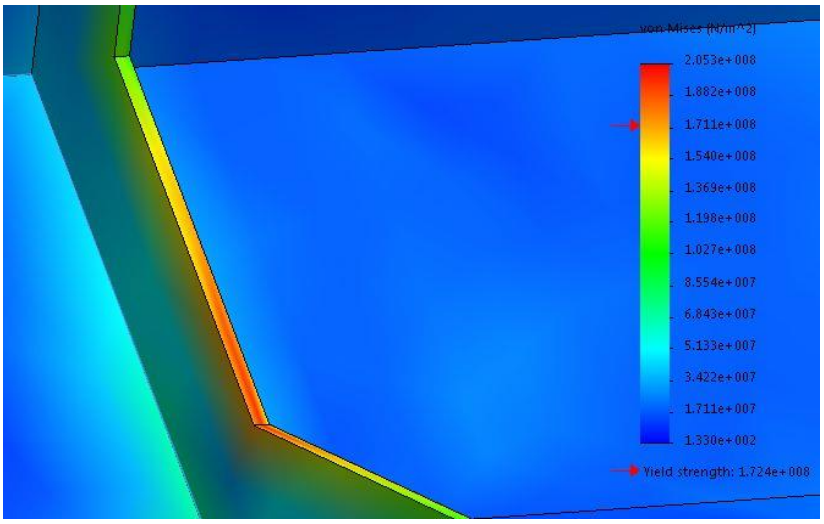

Fig. 3.19 Stress of 4 mm thickness bucket with strengthening elements when force of 26730 N is applied, maximum zone

Fig. 3.20 presents alteration of displacement that occurs on the bucket walls than load of 26730 N is applied. Difference is not significant, only 15 mm.

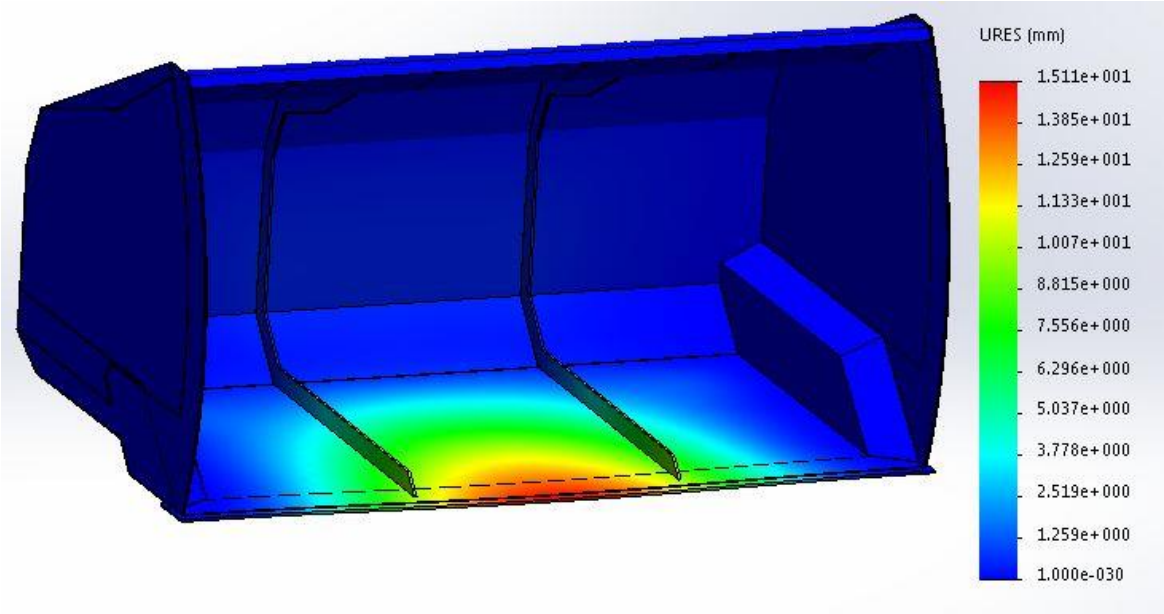

Fig. 3.20 Displacement of 4 mm thickness bucket with strengthening elements when force of 26730 N is applied

To control stresses that exceed yield strength limit, third strengthening element was applied to the drawing. Third element let bucket to sustain the load and not to exceed yield strength limit.

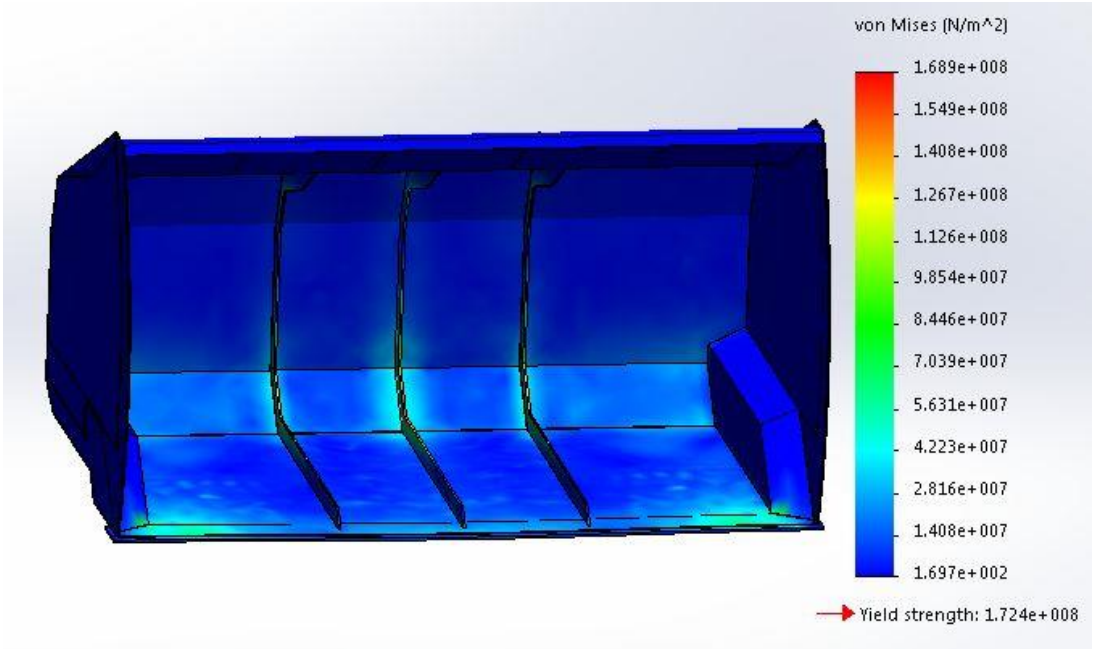

Fig. 3.21 Stress of 4 mm thickness bucket with three strengthening elements when force of 26730 N is applied

From the Fig. 3.22 difference of the mass between A and B is observed. By simplifying the bucket walls to 4 mm thickness we have reduced mass by 180 kg. Third strengthening element weight only 16 kg. So by reducing thickness of the walls and adding strengthening element instead 164 kg was reduced.

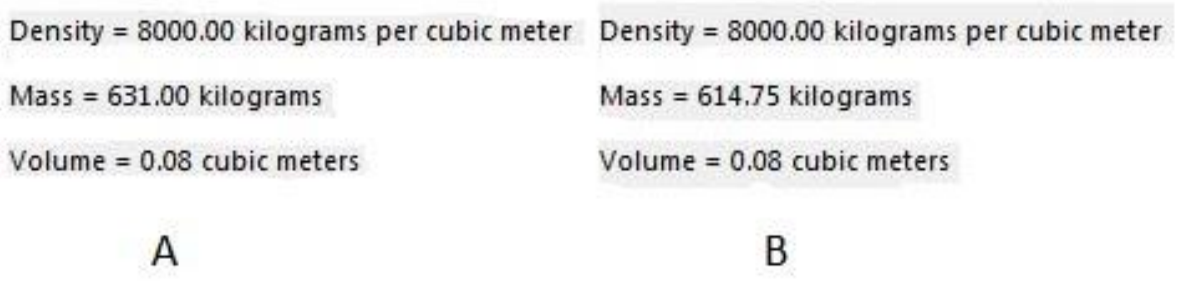

Fig. 3.22 A) mass properties of bucket with 3 strengthening elements B) mass properties of bucket with 2 strengthening elements

Third strengthening element reduced alteration displacement only by 3 mm. No significant change in results was gain here.

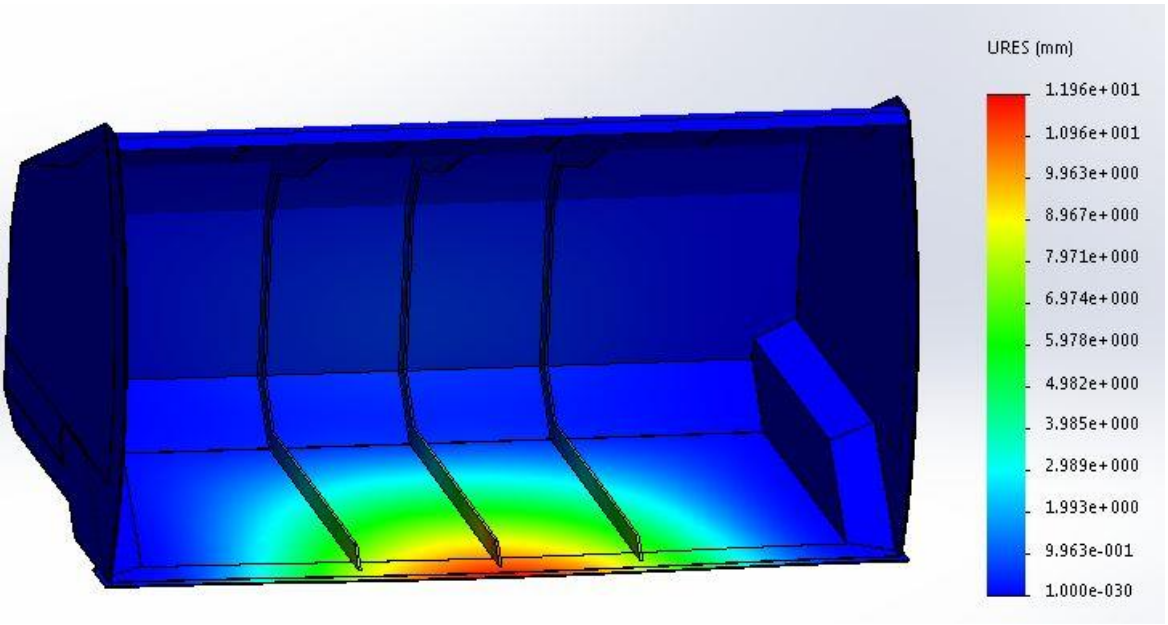

Fig. 3.23 Stress of bucket with three strengthening elements when force of 26730 N is applied

3.8 Bucket of 2 mm thickness steel sheet with load of 26730 N force

Finest thickness of steel sheet that could be used for bucket is 2 mm. Finer sheet of steel could be easily damaged wide range of materials that could occur in operating field. For getting better simulation results three strengthening elements was added. Force of 26730 N represents load of biomass in winter season.

Displacement of surface alters just by 1,2 mm. Thickness of the sheet does not have significant influence for displacement of the bucket.

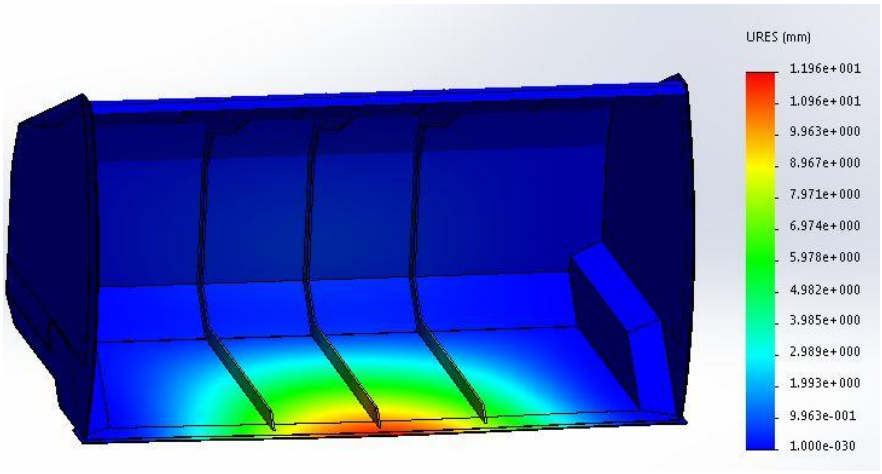

Fig. 3.24 Displacement of 2 mm thickness bucket with three strengthening elements than force of 26730 N is applied

Maximum stress that occurs on the bucket reaches $1{,}595*10^8$ N/m^2 and do not exceed the limit of yield strength of steel.

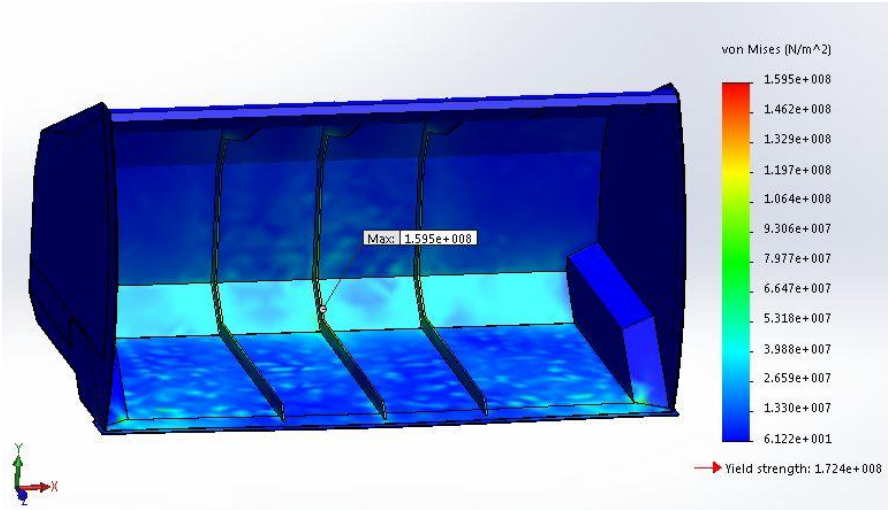

Fig. 3.25 Stress of 2 mm thickness bucket with three strengthening elements than force of 26730 N is applied stress zone

According to gained results bulldozer bucket with 2 mm thickness walls and three strengthening elements is safe to use for transportation of biomass. Mass of newly modelled 2 mm thickness wall bucket is equal to 440 kg see Fig. 3.24. It is 355 kg lighter than universal bucket used by the company.

Mass properties of kausas4mm
Configuration: Default
Coordinate system: -- default --

Density = 8000.00 kilograms per cubic meter

Mass = 440.65 kilograms

Volume = 0.06 cubic meters

Surface area = 34.11 square meters

Center of mass: (meters)
X = 1.40
Y = 0.57
Z = 0.79

Fig. 3.26 Mass properties of 2 mm thickness bucket with three strengthening elements

Force of 525000 N was applied to frond side of the bulldozer bucket blades. Bucket is 2 mm thickness and thickness of the blade is 4 mm wide. During cutting processes 500000 N force will be easily sustained.

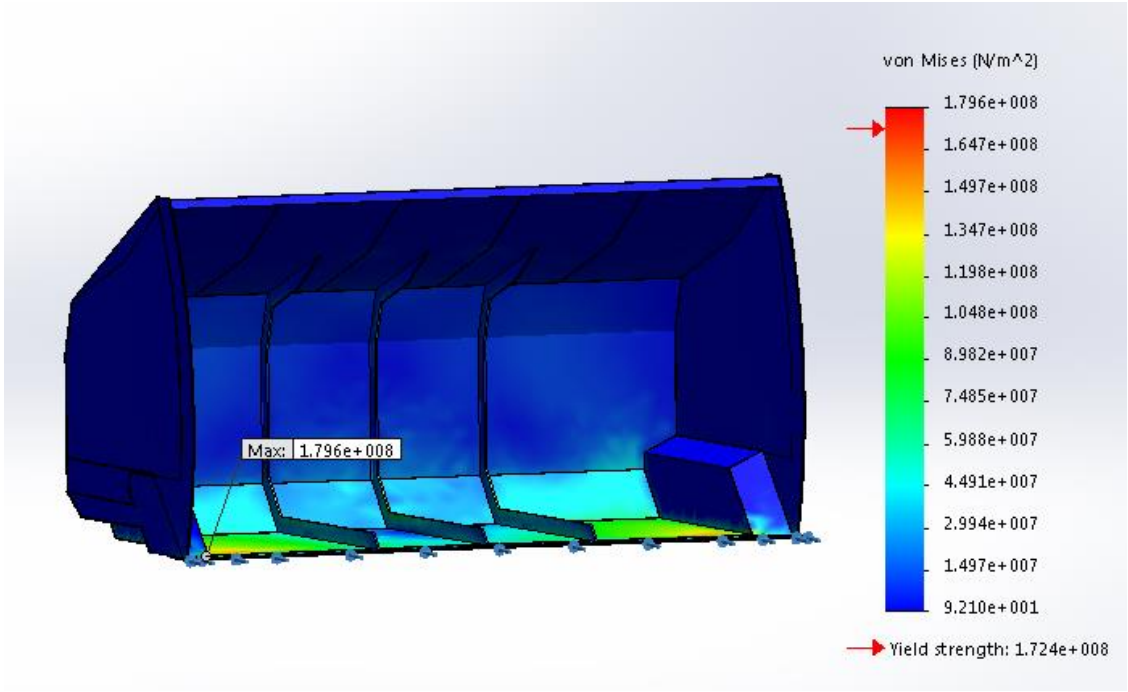

Fig. 3.27 Force of 525000 N applied to front side of the blade

Conclusions

Geomechanics is very innovative field for mechanical researches. To achieve goal of the master work, to optimise geometry of the bucket these objectives were completed:

1. machinery that is used for showing biofuel was analysed;
2. factor that influence density wood pile and other mechanical properties was analysed;
3. static simulation of dozer stresses was made with SolidWorks software;
4. geometry of the bucket was reduced and checked;

Bulldozer bucket geometry was optimized. Static simulation with loads that presents biomass was made. Mass of new bucket was reduced. Surfaces of the bucket sustains the loads. In case company uses bulldozer just for transportation of biomass it is worth to build reduced thickness bucket and operate with less fuel expenses, than use universal Implemex bucket.

References

[1] Official “First Opportunity” biofuel boiler houses page, “About the company”, accessed: 2016.01.06 http://www.firstopportunity.eu/lt/apie-mus.html

[2] Official Case page, ‘CASE sells and supports a full line of construction equipment around the world’, accessed: 2016.01.06 http://www.casece.com/en_us/Equipment/Wheel-Loaders/Pages/621F.aspx

[3] Aleksandro Stulginskio universitetas, Miškų ir Ekologijos fakultetas, Vytautas Mozūras, smulkintos medienos tūrio ir masės tyrimas, magistrantūros baigiamsis darbas accessed 2016.02.07: http://vddb.laba.lt/fedora/get/LT-eLABa-0001:E.02~2010~D_20100621_113541-51165/DS.005.0.02.ETD

[4] Bulk Density – Measurement, Katharine Brown (The University of Western Australia) and Andrew Wherrett (Department of Agriculture and Food, Western Australia) accessed: 2015.05.09 http://soilquality.org.au/factsheets/bulk-density-measurement

[5] P.A. Cundall, O.D.L. Strack, A discrete numerical model for granular assemblies, Geotechnique 29 (1979) 47-65

[6] Momozu M, Oida A, Yamazaki M, Koolen AJ. Simulation of a soilloosening process by means of the modified distinct element method. J. Terramech 2002;39:207–209

[7] Zhang R, Li JQ. Simulation on mechanical behavior of cohesive soil by Distinct Element Method. J Terramech 2006;43:303–16

[8] Gingold, R. A. & Monaghan, J. J. Smoothed particle hydrodynamics - Theory and application to non-spherical stars Monthly Notices of the Royal Astronomical Society, vol. 181, Nov. 1977, p. 375-389

[9] LS-dyna Theory manual, ‘John O. Hallquist, accessed: 2016.01.08 http://www.lstc.com

[10] J.J. Monaghan Smoothed Particle hydrodynamics and Its Diverse Application School of Mathematical Sciences, Monash University, Melbourne, Vic 3800 Australia Vol. 44:323-346

[11] Harlow F, Amsden A. 1975. Numerical calculation of multiphase flow. J. Comput. Phys. 17:19–52

[12] Monaghan JJ, Kocharyan A. 1995. SPH simulation of multiphase flow. Comput. Phys. Commun. 87:225–35

[13] Barriere-Fouchet L, Gonzalez, Murray JR, Humble RJ, Maddison ST. 2005. Dust distribution in protoplanetary disks. Astron. Astrophys. 443:185–94

[14] Ulrich C, Rung T. 2010. SPH modelling of water/soil suspension flows. Presented at SPHERICWorkshop, 5th, Manchester, UK

[15] Capone T, Kajtar JB, Monaghan JJ. 2008. SPH molecules: a model of granular material. Presented at SPHERIC Workshop, 3rd, Lausanne, Switz

[16] Poschel T, Buchholtz V. 1993. Static friction phenomena in granular materials: Coulomb law versus particle geometry. Phys. Rev. Lett. 71:3963–66

[17] C. Ulrich, M. Leonardi, T. Rung, Multi-physics SPH simulation of complex marine-engineering hydrodynamic problems, Ocean Eng. 64 (2013) 109-121.

[18] M.M. Cross, Rheology of non-Newtonian uids: a new ow equation for pseudo-plastic systems, J. Colloid Sci. 20 (1965) 417-437.

[19] A.W. Sisko, The ow of lubricating greases, Ind. En. Chem. 50 (1958) 1789-1792.

[20] K. Szewc, Institute of Fluid-Flow Machinery, Polish Academy of Sciences, Smoothed Particle Hydrodynamics modeling of granular column collapse (2016) 5-6

[21] Utili S, Nova R. DEM analysis of bonded granular geomaterials. Int J Numer Anal Methods 2008;32:1997–2031.